

HyConEx: Hypernetwork classifier with counterfactual explanations

Patryk Marszałek¹, Ulvi Movsum-zada¹, Oleksii Furman², Kamil Książek¹,
Przemysław Spurek¹, and Marek Śmieja¹

¹ Jagiellonian University, Kraków

² University of Science and Technology, Wrocław

marek.smieja@uj.edu.pl

Abstract. In recent years, there has been a growing interest in explainable AI methods. We want not only to make accurate predictions using sophisticated neural networks but also to understand what the model’s decision is based on. One of the fundamental levels of interpretability is to provide counterfactual examples explaining the rationale behind the decision and identifying which features, and to what extent, must be modified to alter the model’s outcome. To address these requirements, we introduce HyConEx, a classification model based on deep hypernetworks specifically designed for tabular data. Owing to its unique architecture, HyConEx not only provides class predictions but also delivers local interpretations for individual data samples in the form of counterfactual examples that steer a given sample toward an alternative class. While many explainable methods generated counterfactuals for external models, there have been no interpretable classifiers simultaneously producing counterfactual samples so far. HyConEx achieves competitive performance on several metrics assessing classification accuracy and fulfilling the criteria of a proper counterfactual attack. This makes HyConEx a distinctive deep learning model, which combines predictions and explainers as an all-in-one neural network. The code is available at <https://github.com/gmum/HyConEx>.

Keywords: Explainable AI · Counterfactual examples · Hypernetworks · Invertible Normalizing Flows · Tabular Data.

1 Introduction

Deep learning has made significant progress in the area of tabular data. It has been shown that recent deep learning models like TabPFN [19], or VisTabNet [39], match or even exceed the performance of state-of-the-art gradient boosting ensembles, such as CatBoost [15] or XGBoost [10]. However, at the cost of increased performance, decisions made by deep learning models cannot be easily explained, which raises concerns regarding trust, accountability, and fairness, especially in critical applications. Instead of designing interpretable

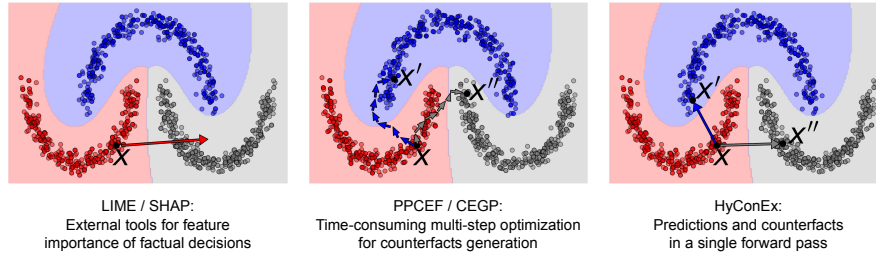


Fig. 1: Comparison of HyConEx with related explainability methods. Feature attribution methods, like LIME or SHAP, deliver static explanations supporting only current decision. External methods for generating counterfactual examples, eg. PPCEF or CEGP, typically perform time-consuming optimization for every input data point. HyConEx enclose predictions and counterfactuals in a single method, which makes it extremely efficient method that delivers dynamic explanation.

deep learning classifiers, which deliver explanations at the prediction stage, most explainable models operate post-hoc, i.e. they are applied externally to classification models to explain their decisions. Although such an approach is generally acceptable since it does not affect classification performance, it is not optimal because we need to construct multiple models, one operating on the output of the other. Moreover, every single explanation method requires time-consuming optimization.

Explanations can be delivered at several levels. For instance, banks due to legal reasons need to explain refusing or granting a loan. These explanations define the importance of input features, which are crucial for making a given decision. On the other hand, a bank customer would like to know what she/he should do to change the bank’s decision [17]. This topic is related to counterfactual explanations informing which features, and to what extent, have to be modified to obtain a desired model output, e.g. getting a loan. Feature importance methods deliver static information about classification (factual decision). In contrast, counterfactual examples are a type of causal reasoning and provide better insight into the dynamic of the classification rule, see Figure 1.

While there exist highly accurate machine learning classifiers for tabular data [15,16,19,21], as well as external methods for generating counterfactual explanations [26,33,38], no existing model combines these two objectives. In this paper, we make a step towards interpretable deep learning and combine the classification power of neural networks with the dynamic interpretability of counterfactual examples. We introduce HyConEx, a type of hypernetwork, which for every input returns a local classifier equipped with *counterfactual vectors* targeting all other classes. In this way, HyConEx not only returns a highly accurate decision but also suggests possible options of how to change that

decision. Enclosing these two features in one model allows us to speed-up the inference and avoid time-consuming optimization of counterfactuals generation, which is common for external counterfactual explainers [38], see Figure 1. To the best of our knowledge, HyConEx is the first deep learning approach having these two features enclosed in one model.

Our experiments demonstrate that HyConEx achieves accuracy competitive to the state-of-the-art methods (Table 1). Moreover, it produces counterfactual explanations for all classes of comparable quality to external counterfactual explainers (Tables 2, 3 and 4). Since counterfactuals are generated jointly with classification scores in a single forward pass, it does not introduce any additional computational overhead, which makes it a preferred choice over external methods that require time-consuming optimization.

2 Related Works

In this section, we review the literature on interpretable classification, categorizing prior work into three main groups: classical interpretable models, post-hoc explanation techniques (including counterfactual methods) and hybrid approaches that integrate interpretability into the model design.

2.1 Classical Interpretable Models

Tabular data are ubiquitous in domains such as finance, medicine, and fraud detection. Traditional models such as logistic regression and decision trees have long been favored for their inherent transparency. Logistic regression [20], for instance, has been extensively studied due to its linear formulation that directly relates feature coefficients to prediction outcomes. Similarly, linear Support Vector Machines (SVMs) [11] offer interpretability through the explicit characterization of support vectors and decision boundaries. Decision trees provide a natural form of explanation by decomposing decisions into a sequence of simple, human-readable rules. However, while tree-based ensemble methods (for example, boosted trees such as XGBoost [10], LightGBM [22], and CatBoost [15]) achieve high predictive performance in tabular data, the aggregated nature of these models often obscures the interpretability of individual decisions, necessitating the use of additional explanation techniques.

2.2 Post-Hoc and Counterfactual Explanations

To mitigate the opacity of high-performing black-box models, several post-hoc explanation techniques have been proposed. Methods such as LIME (Local Interpretable Model-agnostic Explanations) [32] and SHAP (SHapley Additive exPlanations) [25] approximate complex models locally with simpler, interpretable surrogates that assign importance scores to individual features. These approaches have proven effective in providing insights into the local behavior of classifiers, albeit sometimes at the cost of stability and global consistency.

Counterfactual explanation methods have emerged as a complementary paradigm by identifying minimal changes in input features that would alter a model prediction, thus offering actionable insights into how a different outcome might be achieved. These methods can be broadly categorized into endogenous explainers, which generate counterfactuals by selecting or recombining feature values from the existing dataset, and exogenous explainers, which produce counterfactual examples through interpolation or random data generation without the strict constraint of naturally occurring feature values [17]. Early work by Wachter et al. [37] laid the foundation for exogenous methods, and subsequent approaches have enhanced plausibility by imposing constraints such as convex density restrictions proposed by Artelt and Hammer [5], integrating density estimation via normalizing flows as in PPCEF [38], or guiding the search for interpretable counterfactuals with class prototypes as in CEGP [35]. On the endogenous side, the Contrastive Explanations Method (CEM) [12] emphasizes the importance of both pertinent positives and negatives to justify a prediction, an approach further refined by FACE [29], which identifies feasible and actionable modification paths that respect inherent data and decision constraints, and by the Case-Based Counterfactual Explainer (CBCE) [23] that forms explanation cases by pairing similar instances with contrasting outcomes. Although these techniques vary in their mechanisms, they commonly require additional post hoc optimization separate from the classifier.

2.3 Deep Interpretable Models

Deep interpretable models have emerged as a promising avenue to reconcile high predictive performance with intrinsic explainability in tabular data. The early work of Alvarez-Melis and Jaakkola [3] pioneered the idea of self-explaining neural networks that enforce local linearity and stability, laying the groundwork for models that can be interpretable by design. Based on these concepts, attention-based architectures such as TabNet [4] have demonstrated that sequential attention mechanisms can dynamically select the most relevant features during decision-making, offering built-in interpretability alongside competitive accuracy. Later, architectures like the Interpretable Mesomorphic Neural Networks (IMN) [21] leverage deep hypernetworks to generate instance-specific linear models, providing direct feature attributions without compromising the expressive power of deep networks. Complementary approaches include Neural Additive Models (NAMs) [2], which combine the flexibility of deep learning with the transparency of generalized additive models through per-feature shape functions, and Deep Abstract Networks (DANet) [9], which utilize specialized abstract layers to hierarchically group and transform features for clearer semantics.

Collectively, these advances mark a significant evolution in deep interpretable modeling, offering unified frameworks where prediction accuracy and built-in explainability are integrated from the ground up, but none of these methods inherently provides counterfactual explanations, which remain an external, post-hoc addition.

3 HyConEx model

This section describes HyConEx, which is a deep learning classifier equipped with counterfactual explanations. Since HyConEx is an all-in-one neural network, predictions and counterfactuals are returned in a single forward pass. First, we introduce the basic concept of counterfactual explanations. Next, we present two main components of HyConEx: hypernetwork [1] and invertible normalizing flows [31]. Finally, we describe HyConEx model in detail.

3.1 Counterfactual explanations

Counterfactuals aim to explain classifier decisions by examples [36]. They indicate the modifications of the input examples, which are required to flip the classifier decision. In practice, counterfactual examples represent samples generated from the alternative (non-factual) classes, which are similar to the input. By analyzing the difference between input and output examples, we obtain counterfactual explanations.

To describe a basic approach to generating counterfactual examples, let $f : \mathbb{R}^D \rightarrow \mathbb{R}^K$ be a multi-class classifier trained on a given dataset $\{(x_i, y_i)\}_{i=1}^N$, where D denotes the number of input features, K is the number of classes and N is the number of training data. We assume that the classifier f returns a class label y for a data point x . The question is: *how to modify x to obtain an alternative class y' ?* Since we are interested in local decisions, we want to make as small changes to x as possible. Formally, counterfactual example x' can be defined as a solution to the optimization problem [37]:

$$\operatorname{argmin}_{x' \in \mathbb{R}^D} \mathcal{L}(f(x'), y') + C \cdot d(x, x'),$$

where $\mathcal{L}(\cdot, \cdot)$ represents a loss function for classification, $d(\cdot, \cdot)$ is a distance function (proximity measure) acting as a penalty for deviations from the original input x , and $C > 0$ indicates the hyperparameter for regularization intensity.

Contemporary methods satisfy many additional properties, such as sparsity, actionability, or diversity, which increase their interpretation capabilities [36]. In this paper, we are especially interested in constructing plausible counterfactuals [17]. A counterfactual is plausible if it is located within the high-density region of data. This feature distinguishes counterfactuals from adversarial examples. Plausibility is typically assessed via a straightforward k-neighborhood analysis of the counterfactual relative to the original dataset [6]. Recently, PPCEF [38] has employed invertible normalizing flows to evaluate plausibility in tabular data contexts. Our study adopts a similar approach by integrating invertible normalizing flows directly into the classification model.

3.2 Hypernetwork classifiers

Hypernetworks, introduced in [1], are defined as neural models that generate weights for a separate target network that solves a specific task. In this seminal

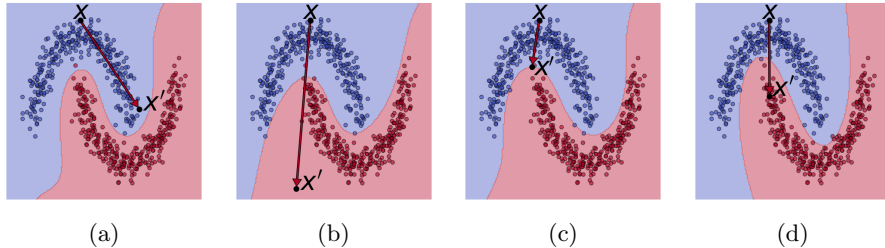


Fig. 2: Illustration of all elements of our cost function: (a) Cross-entropy is applied only to the input example similar to IMN [21]. As we can see, the normal vector w is turned into the target class, but the translation of $x' = x - w$ does not lead to the change of class label; (b) We additionally apply the cross-entropy to the counterfactual example. In this case, we produce strong modification, which does not lead to in-distribution samples; (c) We supply the previous loss with the proximity between input and counterfactual. We observe that the model gives the smallest modification, which changes the class label. (d) Complete loss with plausibility term. The final HyConEx enforces x' to lie in the manifold of the target class.

work, the authors aim to reduce the number of trainable parameters by designing a hypernetwork with fewer parameters than the target network. The hypernetworks were developed and applied in several areas including generative modeling, continual learning [27], image representations [24], and many others[34].

The recently introduced Interpretable Mesomorphic Networks (IMN) [21] uses a hypernetwork to construct an individual local linear classifier for every tabular data point. Due to the linearity of the classifier, IMN delivers the local importance of the input features (determined by the linear model). Although IMN uses local linear models, it produces global non-linear decision boundary in the whole data space.

In this approach, the hypernetwork $H(\cdot; \theta) : \mathbb{R}^D \rightarrow \mathbb{R}^{K \times (D+1)}$ takes a data point $x \in \mathbb{R}^D$ and outputs the local linear classifier for K -class problem given by the weight matrix $W = H(x; \theta)$. The k -th row of W determines the logit of the k -th class:

$$z(x; W)_k = \sum_{d=1}^D W_{k,d} x_d + W_{k,0}.$$

In consequence, the probability that x belongs to k -th class equals:

$$f(x; W)_k = \frac{\exp(z(x; W)_k)}{\sum_{j=1}^K \exp(z(x; W)_j)}.$$

The hypernetwork is instantiated by Tabular ResNet [21].

Let us observe that the linear model determined by $W = H(x; \theta)$ contains the local normal vectors to the linear classification boundary for the input x .

In other words, it gives a direction to the decision boundary, see Figure 2a, which can be understood as *feature importance* vector for x . Unfortunately, these vectors represent a chosen class against all other outcomes. Our study focuses on generating counterfactual examples in a single forward pass, which provides more profound insights.

3.3 Invertible Normalizing Flows

To generate plausible counterfactuals, we use invertible normalizing flows (INFs) to model the density of each class [31].

INFs can be seen as sophisticated tools for estimating data density. In practice, INFs integrate autoencoder structures where the encoder is an invertible function. Due to these characteristics, the inverse function can serve as a decoder. These models do not reduce dimensionality, making them generally suitable for representing relatively low- or medium-dimensional data. This makes them particularly well-suited for handling tabular data. INFs are trained using negative log-likelihood (NLL) as a cost function.

INFs transform a latent variable z with a known prior distribution $p(z)$ into an observed space variable x with an unknown distribution. This transformation is modeled by a series of invertible (parametric) functions:

$$x = F(x) = f_K \circ \dots \circ f_1(z).$$

To model a separate density for each class, INF is additionally conditioned by a class vector y . In this case, the conditional log-likelihood for x is expressed as:

$$\log p_F(x|y) = \log p(z) - \sum_{k=1}^K \log \left| \det \frac{\partial f_k}{\partial z_{k-1}} \right|,$$

where $z = f_1^{-1} \circ \dots \circ f_K^{-1}(x, y)$ is a result of the invertible mapping. A significant challenge in INFs is the selection of appropriate invertible functions, denoted as f_K, \dots, f_1 . The existing literature presents a variety of solutions to address this issue, with notable methodologies including NICE [13], RealNVP [14], and MAF [28].

3.4 HyConEx architecture

Our architecture comprises two key elements: hypernetwork classifier and invertible normalizing flows, see Figure 3. By defining a proper loss function and designing dedicated training procedure, the generated classifier delivers predictions and the associated counterfactual explanations.

Let us construct a hypernetwork $H(\cdot; \theta)$, which returns a weight matrix $W = H(x; \theta)$ that defines a local linear classifier $f(\cdot; W)$ as described in Section 3.2. We will force the hypernetwork to produce such a weight matrix W , which not only contains information needed for class predictions but also gives the localization of counterfactual examples for alternative classes. To keep our

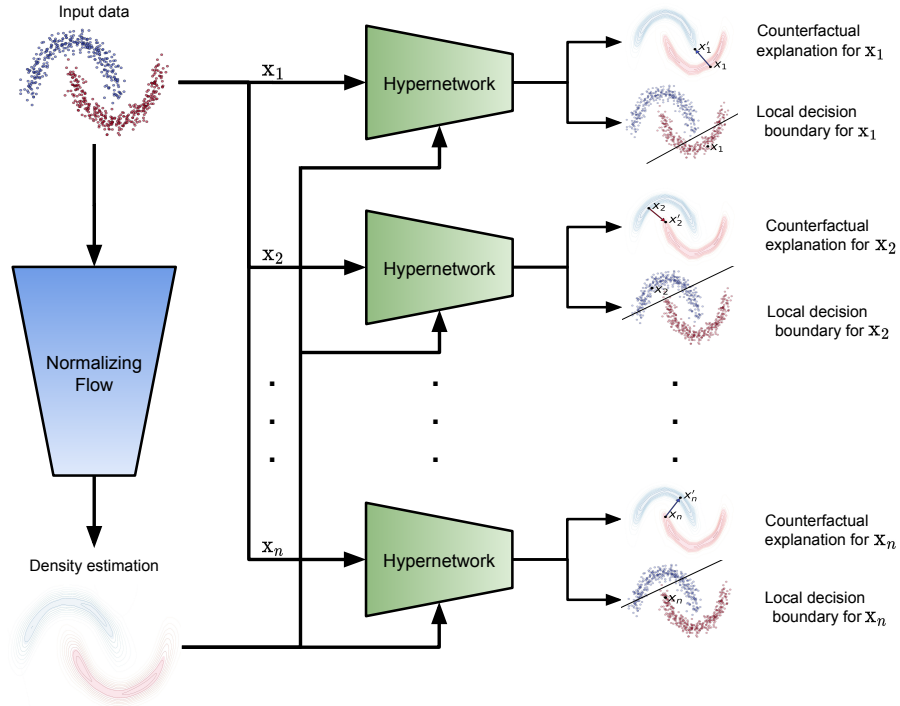


Fig. 3: Illustration of HyConEx architecture. The hypernetwork takes every input together with the estimated data density and returns: (1) local decision boundary, and (2) counterfactual examples for all alternative classes. In consequence, we obtain predictions and counterfactuals in a single forward pass. We emphasize that HyConEx uses a single hypernetwork, which was duplicated here into n models for illustration only.

model as simple as possible, we do not introduce any additional parameters. The counterfactual examples will be determined by the rows of weight matrix W .

To explain our approach, we assume that $x \in \mathbb{R}^D$ was classified by $f(x; W)$ as the element of the class k . It means that the k -th row of W is related to the vector that is normal to the local decision boundary generated for x . To localize the counterfactual examples of alternative classes, we employ the remaining rows of W . More precisely, the translation of x by the m -th row W_m , defined by $x' = x - W_m$, has to point out the counterfactual example of the class m . To satisfy this requirement, we need to ensure that x' :

1. is classified by f as the element of m -th class,
2. is close to the original input x ,
3. is plausible (in-distribution sample).

First, the correct class prediction of x' is forced by minimizing the cross-entropy loss, $\mathcal{L}(f(x'; W), m)$ using our hypernetwork classifier $W = H(x'; \theta)$, see Figure 2b. Second, to satisfy the proximity between x and x' , we minimize the MSE between them, i.e. $\|x - x'\|^2$, see Figure 2c. Third, the plausibility is obtained using class conditional INFs. More precisely, we train class conditional INF, $F(x|y; \phi)$, to model the density of each class. Next, we adjust the counterfactual example x' to align with a fixed value of the estimated data density, see Figure 2d. In our paper, we follow the PPCEF [38] approach and put:

$$\mathcal{L}_F(x', m) = \max(\delta - p_F(x'|m), 0),$$

where $p_F(x'|m)$ denotes the class conditional probability of the counterfactual explanation x' under the desired target class value m and δ represents the density threshold.

The complete loss function of HyConEx combines the above three loss terms with the cross-entropy of the original input x to provide the correct classification. Since we are interested in generating counterfactual examples for all alternative classes, we iterate over all classes. Let us first define the counterfactual loss for m -th class:

$$\mathcal{L}_{conEx}(x, m; \theta, \phi) = \alpha_1 \mathcal{L}(f(x'; W), m) + \alpha_2 \|x - x'\| + \alpha_3 L_F(x', m),$$

where $x' = x - W_m$ and α_i 's are regularization hyperparameters. Then our final loss equals:

$$\mathcal{L}_{HyConEx}(x, y; \theta, \phi) = \mathcal{L}(f(x), y) + \sum_{m \neq y} \mathcal{L}_{conEx}(x, m; \theta, \phi).$$

3.5 Initialization and training process of HyConEx

Training of HyConEx involves training of hypernetwork $H(\cdot; \theta)$ together with conditional INF, $F(\cdot; \phi)$. For stability, we first pre-train both networks as described below.

Since the hypernetwork produces not only a classification boundary but also counterfactual explanations, we cannot pre-train the hypernetwork only with a typical cross-entropy loss. For the hypernetwork to be aware of the closest elements of opposite classes, we apply the clustering of each class separately using the k-means algorithm [8]. Then we combine the classification cross-entropy loss $\mathcal{L}(f(x), y)$ with the proximity loss between counterfactual candidate x' and the nearest clustering mean of the alternative class:

$$\mathcal{L}(f(x), y) + \alpha \sum_{m \neq y} \|x' - r_m\|$$

where $x' = W_m$ and r_k is the closest cluster center from the k -th class to a data point x and α is a hyperparameter. This clustering-based pre-training is also targeted to obtain plausible counterfactuals, but with lower quality than

applying INFs. However, it is more stable which is important at the initial stage of the training.

We also train a conditional INF $F(\cdot; \phi)$ on class labels predicted by a pre-trained hypernetwork classifier. This initialization helps to stabilize the training process and leads to faster convergence.

After pre-training stage, we freeze the parameters of INF and train only the hypernetwork network until the convergence.

4 Experiments

We evaluate HyConEx in terms of classification accuracy and counterfactual explanation quality. To our knowledge, HyConEx is the first deep learning model that learns to return counterfactual examples by a classification model itself.

4.1 Instantiation of HyConEx

For implementing HyConEx, we use TabResNet as hypernetwork backbone and MAF as conditional INF. TabResNet uses 4 residual blocks, a hidden size of 256, and a dropout rate of 0.25. MAF is configured with 16 hidden features, 8 layers, and 4 blocks per layer.

The initialization phase uses trade-off parameter $\alpha = 0.8$ and is continued until model convergence. In the second phase, we employ the same Adam optimizer and cosine annealing scheduler as used during pre-training. For all experiments, we linearly increase the trade-off parameters α_i from 0 to $\alpha_1=0.8$, $\alpha_2=0.1$ and $\alpha_3=0.1$. The duration of the second phase is determined using early stopping, which aims to maximize plausibility while ensuring high model accuracy, high counterfactual validity, and low proximity.

4.2 Predictive performance

To validate the predictive performance of HyConEx, we use the benchmark from [21]. More precisely, we compare HyConEx with strong ensemble methods (Random Forest and CatBoost), classical shallow classifiers (decision trees, logistic regression) as well as deep learning models equipped with interpretability tools (TabNet [4], TabResNet, IMN [2]). We use 18 tabular datasets retrieved from OpenML repository of varied characteristics (see Table 1 for datasets IDs). We report AUROC (Area Under the Receiver Operating Characteristic curve), which is well suited for imbalanced data as well.

The results presented in Table 1 demonstrate that HyConEx maintains competitive performance compared to state-of-the-art methods, achieving the highest AUROC on several datasets (31, 1067, 1464, 1468). In particular, HyConEx shows comparable performance to TabResNet and CatBoost, suggesting that the additional counterfactual generation capability does not compromise classification accuracy. This confirms that our model effectively preserves predictive performance while gaining interpretability through counterfactual explanations.

Table 1: Comparison of predictive performance using AUROC measure.

Dataset ID	Decision Tree	Logistic Regression	Random Forest	TabNet	TabResNet	CatBoost	IMN	HyConEx
3	0.987	0.990	0.998	0.983	0.999	0.999	0.999	0.997
12	0.938	0.999	0.998	0.995	0.999	0.999	0.999	0.999
31	0.643	0.775	0.795	0.511	0.756	0.790	0.751	0.799
54	0.804	0.938	0.927	0.501	0.968	0.934	0.957	0.946
1067	0.620	0.802	0.801	0.789	0.808	0.800	0.805	0.809
1461	0.703	0.908	0.930	0.926	0.931	0.937	0.930	0.905
1464	0.599	0.749	0.666	0.516	0.740	0.709	0.742	0.769
1468	0.926	0.996	0.995	0.495	0.995	0.996	0.994	0.996
1486	0.935	0.987	0.993	0.991	0.994	0.994	0.993	0.987
1489	0.842	0.805	0.962	0.928	0.949	0.948	0.950	0.900
1590	0.752	0.903	0.917	0.908	0.915	0.930	0.915	0.872
40984	0.946	0.980	0.995	0.985	0.994	0.995	0.994	0.985
41142	0.626	0.742	0.796	0.713	0.782	0.822	0.775	0.725
41143	0.749	0.850	0.880	0.823	0.860	0.870	0.865	0.835
41146	0.910	0.966	0.983	0.974	0.982	0.988	0.981	0.979
41161	0.857	0.995	0.999	0.997	0.998	1.000	0.998	0.994
41163	0.873	0.994	0.999	0.998	1.000	1.000	1.000	0.992
41164	0.786	0.898	0.925	0.888	0.913	0.935	0.902	0.895

4.3 Counterfactual explanations

We evaluated counterfactual explanations by assessing the quality, plausibility, and computational efficiency of our HyConEx method compared to established baselines such as CEM [12], CBCE [23], CEGP [35], and PPCEF [38]. Our evaluation leverages datasets from the PPCEF benchmark [38] and expands the original PPCEF setup by incorporating additional categorical datasets. We consider multiple scenarios, including binary classification using datasets such as *Moons*, *Law*, *Audit* and *Heloc*, multiclass classification using datasets such as *Blobs*, *Digits* and *Wine*, and cases with categorical features using *Adult* [7], *Credit-A* [30] and *Credit-G* [18] datasets. For all experiments, we perform standard preprocessing: normalizing features and handling class imbalance via downsampling. For datasets with categorical features we introduce slight Gaussian noise to labels for efficient training, while for counterfactual examples, we apply softmax activation to produce one-hot predictions and select the class with maximum value.

Since HyConEx is an interpretable model, which includes predictions and counterfactuals in one model, all methods generate counterfactuals for HyConEx classifier. In this way, we provide a fair comparison of all methods. The test AUROC of HyConEx for all datasets equals: Audit auroc=0.995, Credit-A auroc=0.932, Credit-G auroc=0.794, Moons auroc=1.000, Law auroc=0.834, Heloc auroc=0.798, Adult auroc=0.872, Wine auroc=1.000, Blobs auroc=1.000, Digits auroc=0.995.

Metrics We quantify counterfactual quality using several metrics. Coverage (Cover.) indicates the fraction of instances for which counterfactuals are generated, while Validity (Valid.) represents the percentage of counterfactuals that successfully changed the model prediction to the desired target. To assess the

Table 2: Comparative Results for Binary Classification Datasets

Dataset	Method	Cover.↑	Valid.↑	L1↓	L2 ↓	P.Plaus.↑	LogDens↑	LOF↓	IsoForest↑	Time(s)↓
Moons	CBCE	1.00	1.000	0.576	0.459	1.000	2.11	0.963	0.033	0.75
	CEGP	1.00	1.000	0.190	0.154	0.000	-2.39	1.379	-0.0006	4485.89
	CEM	0.99	1.000	0.543	0.508	0.059	-6.740	1.786	-0.077	2752.94
	WACH	0.99	0.975	0.208	0.178	0.000	-1.921	1.300	-0.001	2724.99
	PPCEF	1.00	1.000	0.337	0.261	0.990	1.32	1.032	0.022	35.62
	HyConEx	1.00	1.000	0.502	0.409	1.000	1.93	0.985	0.033	0.003
Law	CBCE	1.00	1.000	0.895	0.597	0.493	-0.45	1.219	-0.024	1.73
	CEGP	1.00	1.000	0.204	0.170	0.457	0.95	1.042	0.049	10155.25
	CEM	0.99	1.000	0.310	0.297	0.518	1.19	1.088	0.005	5491.65
	WACH	1.00	0.995	0.412	0.341	0.511	1.16	1.084	-0.002	5579.35
	PPCEF	1.00	1.000	0.338	0.202	1.000	1.83	1.032	0.067	131.00
	HyConEx	1.00	1.000	0.359	0.227	0.894	2.54	1.026	0.060	0.005
Audit	CBCE	1.00	1.000	3.128	1.496	1.000	51.90	1.031	0.097	0.46
	CEGP	1.00	1.000	0.148	0.081	0.164	27.17	1.576	0.085	2578.10
	CEM	1.00	1.000	0.145	0.126	0.050	-23.41	1.620	0.083	1502.50
	WACH	1.00	1.000	0.232	0.158	0.016	-51.49	1.545	0.075	1586.24
	PPCEF	1.00	1.000	0.805	0.246	1.000	52.87	1.452	0.095	22.87
	HyConEx	1.00	0.975	0.495	0.151	0.615	58.30	1.484	0.068	0.003
Heloc	CBCE	1.00	1.000	3.524	1.084	1.000	32.27	0.989	0.056	11.15
	CEGP	1.00	1.000	0.027	0.022	0.428	30.19	1.073	0.059	42475.70
	CEM	1.00	1.000	0.0447	0.043	0.361	28.86	1.079	0.053	25924.86
	WACH	1.00	0.998	0.345	0.193	0.031	-49.78	1.189	0.025	26430.91
	PPCEF	1.00	0.993	0.457	0.124	0.999	34.93	1.042	0.074	486.02
	HyConEx	1.00	0.997	0.416	0.142	0.602	34.61	1.073	0.065	0.019

minimality of the changes from the original example, we report the L1 and L2 norms for continuous features and Hamming distance for categorical features. Plausibility is measured using a probabilistic plausibility score (P.Plaus.) which indicates how many counterfactuals have an estimated log density higher than the median log density of the train set. Furthermore, we provide density metrics such as log density (LogDens) and outlier detection scores such as Local Outlier Factor (LOF) and Isolation Forest (IsoForest). Finally, we report the CPU computation time in seconds to generate counterfactuals to capture the efficiency of the method.

Results Our experiments demonstrate that HyConEx consistently achieves near-perfect coverage and validity across diverse settings while offering substantial computational advantages. Results presented in Table 2 show that for binary classification tasks, our method generates counterfactual explanations with competitive proximity metrics and high plausibility, processing the moons dataset in merely 0.003 seconds compared to 0.75 seconds for CBCE. This pattern extends to multiclass scenarios as shown in Table 3 and datasets with categorical features as illustrated in Table 4, where HyConEx maintains strong performance while producing valid counterfactuals that require only minimal modifications and remain within high-density regions of the training data distribution. By providing counterfactual explanations that are both valid and plausible, our approach enhances the practical interpretability and actionability of explanations while significantly outperforming baseline methods in computation speed, demonstrating

Table 3: Comparative Results for Multi-Class Datasets (averaged over all classes)

Dataset	Method	Cover.↑	Valid.↑	L1↓	L2↓	P.Plaus.↑	LogDens↑	LOF↓	IsoForest↑	Time(s)↓
Blobs	CBCE	1.00	1.000	0.764	0.581	0.333	1.03	1.31	-0.029	0.92
	CEGP	0.98	1.000	0.370	0.303	0.000	-9.35	2.625	-0.076	4607.08
	WACH	0.99	0.993	0.393	0.341	0.000	-8.650	2.756	-0.081	2380.44
	PPCEF	1.00	1.000	0.675	0.500	1.000	2.26	1.162	0.007	26.74
	HyConEx	1.00	1.000	0.701	0.527	0.943	2.88	1.058	0.028	0.004
Digits	CBCE	1.00	1.000	15.448	3.002	0.330	53.65	1.073	0.029	1.80
	CEGP	0.96	1.000	6.090	1.423	0.011	-392.35	1.201	-0.023	8165.49
	WACH	1.00	1.000	2.076	0.999	0.018	-69.30	1.097	0.005	4354.78
	PPCEF	1.00	1.000	6.550	1.130	1.000	55.98	1.055	0.029	86.34
	HyConEx	1.00	0.999	6.978	1.396	0.809	62.98	1.051	0.040	0.005
Wine	CBCE	1.00	1.000	3.560	1.178	0.667	7.25	1.062	0.037	0.11
	CEGP	1.00	1.000	1.346	0.547	0.000	-10.70	1.174	0.005	544.26
	WACH	1.00	1.000	1.010	0.625	0.015	-12.379	1.228	0.005	287.38
	PPCEF	1.00	1.000	1.959	0.600	1.000	7.38	1.033	0.064	8.12
	HyConEx	1.00	1.000	2.241	0.738	0.700	8.40	0.999	0.054	0.001

its effectiveness for counterfactual analysis across binary, multiclass, and categorical tabular data.

Table 4: Comparative Results for Datasets with Categorical Features

Dataset	Method	Cover.↑	Valid.↑	L2↓	Ham.↓	P.Plaus.↑	LogDens↑	LOF↓	IsoForest↑	Time(s)↓	
Adult	CBCE	1.00	1.000	0.334	0.652	0.751	30.79	0.999	-0.002	88.53	
	CEGP	0.43	0.999	0.313	0.000	0.432	25.05	1.777	0.037	67348.95	
	PPCEF	1.00	0.672	0.379	0.249	0.646	27.14	1.599	0.031	1453.48	
	HyConEx	1.00	1.000	0.136	0.328	0.861	29.86	1.257	0.037	0.05	
	Credit-G	CBCE	1.00	1.000	0.944	0.584	0.517	18.83	1.007	0.014	0.51
Credit-G	CEGP	1.00	1.000	0.311	0.026	0.258	0.45	1.029	0.024	3035.62	
	PPCEF	1.00	0.517	0.387	0.005	0.358	4.69	1.023	0.026	23.45	
	HyConEx	1.00	1.000	0.585	0.067	0.492	8.51	1.022	0.031	0.003	
	Credit-A	CBCE	1.00	1.000	7.675	0.486	0.478	10.478	1.208	0.002	0.58
		CEGP	0.96	1.000	0.372	0.000	0.106	7.888	1.048	0.029	3415.51
PPCEF		1.00	0.355	0.669	0.082	0.167	13.853	1.040	0.039	29.94	
HyConEx		1.00	1.000	1.606	0.164	0.638	21.749	1.055	0.040	0.003	

4.4 Ablation Study

To evaluate the contribution of each loss component, we performed an ablation study on the *Heloc* dataset. Table 5 reports the performance metrics for the following loss configurations:

- **Base**: The loss contains only the cross-entropy of the input data, which fails to produce valid counterfactuals.
- **Base+CE**: Augments the base loss with a cross-entropy (CE) term for counterfactual example. This setup achieves perfect validity but yields counterfactuals with poor plausibility and highly negative log density values, suggesting out-of-distribution samples.

- **Base+CE+Flow**: Adds a flow constraint to the Base+CE loss to encourage plausibility. It retains perfect validity while significantly boosting plausibility.
- **Base+CE+Dist**: Integrates a distance minimization (Dist) term with the Base+CE loss to enforce proximity, leading to a dramatic reduction in L1 and L2 distances at the cost of a slight decrease in validity.
- **Full**: Combines all components (CE, Flow, and Dist) to balance validity, proximity, and plausibility.

The results demonstrate that each component contributes to the quality of generated counterfactuals, with the full model effectively balancing the trade-offs.

Table 5: Ablation Study: Importance of Loss Components on the Heloc Dataset. Best results are in **bold** and the second best are underlined.

Loss Type	Cover.↑	Valid.↑	L1↓	L2↓	P.Plaus.↑	LogDens↑	LOF↓	IsoForest↑
Base	1.00	0.000	-	-	-	-	-	-
Base+CE	1.00	1.000	6.394	1.628	0.000	-34761532.00	3.925	-0.036
Base+CE+Flow	1.00	1.000	1.461	0.475	0.662	33.707	1.108	0.058
Base+CE+Dist	1.00	0.988	0.098	0.032	0.394	27.66	1.072	0.060
Full	1.00	<u>0.997</u>	<u>0.416</u>	<u>0.142</u>	<u>0.602</u>	34.61	<u>1.073</u>	0.065

5 Conclusion

Understanding model decisions is crucial in explainable AI, mainly through counterfactual explanations highlighting key feature modifications affecting predictions. While existing methods generate counterfactuals for external models, no interpretable classifier has produced predictions and counterfactuals simultaneously. We introduced HyConEx, a deep hypernetwork-based model tailored for tabular data, which provides accurate classifications and generates counterfactual examples within high-density class regions. Our approach achieves competitive performance while ensuring interpretability, making HyConEx a unique all-in-one neural network that seamlessly integrates prediction and explanation.

References

1. Hypernetworks. arXiv preprint arXiv:1609.09106 (2016)
2. Agarwal, R., Melnick, L., Frosst, N., Zhang, X., Lengerich, B., Caruana, R., Hinton, G.E.: Neural additive models: Interpretable machine learning with neural nets. *Advances in neural information processing systems* **34**, 4699–4711 (2021)
3. Alvarez Melis, D., Jaakkola, T.: Towards robust interpretability with self-explaining neural networks. *Advances in neural information processing systems* **31** (2018)
4. Arik, S., Pfister, T.: Tabnet: Attentive interpretable tabular learning. *Proceedings of the AAAI Conference on Artificial Intelligence* **35**, 6679–6687 (05 2021). <https://doi.org/10.1609/aaai.v35i8.16826>

5. Artelt, A., Hammer, B.: Convex density constraints for computing plausible counterfactual explanations. In: International conference on artificial neural networks. pp. 353–365. Springer (2020)
6. Augustin, M., Boreiko, V., Croce, F., Hein, M.: Diffusion visual counterfactual explanations. *Advances in Neural Information Processing Systems* **35**, 364–377 (2022)
7. Becker, B., Kohavi, R.: Adult. UCI Machine Learning Repository (1996), DOI: <https://doi.org/10.24432/C5XW20>
8. Burkardt, J.: K-means clustering. Virginia Tech, Advanced Research Computing, Interdisciplinary Center for Applied Mathematics p. 5 (2009)
9. Chen, J., Liao, K., Wan, Y., Chen, D.Z., Wu, J.: Danets: Deep abstract networks for tabular data classification and regression. In: Proceedings of the AAAI Conference on Artificial Intelligence. vol. 36, pp. 3930–3938 (2022)
10. Chen, T., Guestrin, C.: Xgboost: A scalable tree boosting system. In: Proceedings of the 22nd acm sigkdd international conference on knowledge discovery and data mining. pp. 785–794 (2016)
11. Cortes, C., Vapnik, V.: Support-vector networks. *Machine learning* **20**(3), 273–297 (1995)
12. Dhurandhar, A., Chen, P.Y., Luss, R., Tu, C.C., Ting, P., Shanmugam, K., Das, P.: Explanations based on the missing: Towards contrastive explanations with pertinent negatives. *Advances in neural information processing systems* **31** (2018)
13. Dinh, L., Krueger, D., Bengio, Y.: Nice: Non-linear independent components estimation. *arXiv preprint arXiv:1410.8516* (2014)
14. Dinh, L., Sohl-Dickstein, J., Bengio, S.: Density estimation using real nvp. *arXiv preprint arXiv:1605.08803* (2016)
15. Dorogush, A.V., Ershov, V., Gulin, A.: Catboost: gradient boosting with categorical features support. In: Workshop on ML Systems at Advances in Neural Information Processing Systems (2017)
16. Gorishniy, Y., Rubachev, I., Khrulkov, V., Babenko, A.: Revisiting deep learning models for tabular data. In: Beygelzimer, A., Dauphin, Y., Liang, P., Vaughan, J.W. (eds.) *Advances in Neural Information Processing Systems* (2021)
17. Guidotti, R.: Counterfactual explanations and how to find them: literature review and benchmarking. *Data Mining and Knowledge Discovery* **38**, 2770–2824 (2024). <https://doi.org/10.1007/s10618-022-00831-6>
18. Hofmann, H.: Statlog (German Credit Data). UCI Machine Learning Repository (1994), DOI: <https://doi.org/10.24432/C5NC77>
19. Hollmann, N., Müller, S., Eggenberger, K., Hutter, F.: TabPFN: A transformer that solves small tabular classification problems in a second. In: International Conference on Learning Representations 2023 (2023)
20. Hosmer Jr, D.W., Lemeshow, S., Sturdivant, R.X.: Applied logistic regression. John Wiley & Sons (2013)
21. Kadra, A., Arango, S.P., Grabocka, J.: Interpretable mesomorphic networks for tabular data. In: The Thirty-eighth Annual Conference on Neural Information Processing Systems (2024)
22. Ke, G., Meng, Q., Finley, T., Wang, T., Chen, W., Ma, W., Ye, Q., Liu, T.Y.: Lightgbm: a highly efficient gradient boosting decision tree. In: Proceedings of the 31st International Conference on Neural Information Processing Systems. p. 3149–3157. NIPS’17, Curran Associates Inc., Red Hook, NY, USA (2017)
23. Keane, M.T., Smyth, B.: Good counterfactuals and where to find them: A case-based technique for generating counterfactuals for explainable ai (xai). In: Case-

- Based Reasoning Research and Development: 28th International Conference, IC-CBR 2020, Salamanca, Spain, June 8–12, 2020, Proceedings 28. pp. 163–178. Springer (2020)
24. Klocek, S., Maziarka, L., Wolczyk, M., Tabor, J., Nowak, J., Śmieja, M.: Hypernetwork functional image representation. In: International Conference on Artificial Neural Networks. pp. 496–510. Springer (2019)
 25. Lundberg, S.M., Lee, S.I.: A unified approach to interpreting model predictions. In: Proceedings of the 31st International Conference on Neural Information Processing Systems. p. 4768–4777. NIPS’17, Curran Associates Inc., Red Hook, NY, USA (2017)
 26. Mothilal, R.K., Sharma, A., Tan, C.: Explaining machine learning classifiers through diverse counterfactual explanations. In: Proceedings of the 2020 Conference on Fairness, Accountability, and Transparency. pp. 607–617 (2020)
 27. von Oswald, J., Henning, C., Grewe, B.F., Sacramento, J.: Continual learning with hypernetworks. In: 8th International Conference on Learning Representations (ICLR 2020)(virtual). International Conference on Learning Representations (2020)
 28. Papamakarios, G., Pavlakou, T., Murray, I.: Masked autoregressive flow for density estimation. *Advances in neural information processing systems* **30** (2017)
 29. Poyiadzi, R., Sokol, K., Santos-Rodriguez, R., De Bie, T., Flach, P.: Face: feasible and actionable counterfactual explanations. In: Proceedings of the AAAI/ACM Conference on AI, Ethics, and Society. pp. 344–350 (2020)
 30. Quinlan, R.: Statlog (Australian Credit Approval). UCI Machine Learning Repository (1987), DOI: <https://doi.org/10.24432/C59012>
 31. Rezende, D., Mohamed, S.: Variational inference with normalizing flows. In: International conference on machine learning. pp. 1530–1538. PMLR (2015)
 32. Ribeiro, M.T., Singh, S., Guestrin, C.: "why should i trust you?": Explaining the predictions of any classifier. p. 1135–1144. KDD '16, Association for Computing Machinery, New York, NY, USA (2016)
 33. Ribeiro, M.T., Singh, S., Guestrin, C.: Anchors: high-precision model-agnostic explanations. In: Proceedings of the Thirty-Second AAAI Conference on Artificial Intelligence and Thirtieth Innovative Applications of Artificial Intelligence Conference and Eighth AAAI Symposium on Educational Advances in Artificial Intelligence. AAAI’18/IAAI’18/EAAI’18, AAAI Press (2018)
 34. Sendera, M., Przewięźlikowski, M., Karanowski, K., Zięba, M., Tabor, J., Spurek, P.: Hypershot: Few-shot learning by kernel hypernetworks. In: Proceedings of the IEEE/CVF winter conference on applications of computer vision. pp. 2469–2478 (2023)
 35. Van Looveren, A., Klaise, J.: Interpretable counterfactual explanations guided by prototypes. In: Joint European Conference on Machine Learning and Knowledge Discovery in Databases. pp. 650–665. Springer (2021)
 36. Verma, S., Dickerson, J., Hines, K.: Counterfactual explanations for machine learning: A review. *arXiv preprint arXiv:2010.10596* **2**(1), 1 (2020)
 37. Wachter, S., Mittelstadt, B., Russell, C.: Counterfactual explanations without opening the black box: Automated decisions and the gdpr. *Harv. JL & Tech.* **31**, 841 (2017)
 38. Wielopolski, P., Furman, O., Stefanowski, J., Zięba, M.: Probabilistically plausible counterfactual explanations with normalizing flows. *European Conference on Artificial Intelligence* (2024), <https://api.semanticscholar.org/CorpusID:270067988>
 39. Wydmański, W., Movsum-zada, U., Tabor, J., Śmieja, M.: Vistabnet: Adapting vision transformers for tabular data. *arXiv preprint arXiv:2501.00057* (2024)